



RESEARCH ARTICLE

Antibacterial Activity of Silver Nanoparticles Prepared from *Camellia Sinensis* Extracts in Multi-Drug Resistant *Pseudomonas aeruginosa*

Rami Altameemi¹, Ahmed Harbi AL-Azawi^{2*}, Hawazen Haleem Salih³^{1,2,3}Genetic Engineering and Biotechnology Institute for post graduate studies, University of Baghdad, Baghdad, Iraq

ARTICLE INFO	ABSTRACT
Received: May 21, 2024 Accepted: Jun 28, 2024	The purpose of this study to synthesize and characterize silver nanoparticles using phenolic compounds obtained from <i>Camellia sinensis</i> , to test the antibacterial properties of biosynthesized nanoparticles on the formation of biofilms in multidrug-resistant <i>Pseudomonas aeruginosa</i> . Ten isolates of <i>P. aeruginosa</i> were obtained from the Genetic Engineering and Biotechnology Institute laboratories of the University of Baghdad. By using the VITEK-2 system and culturing the isolates on cetrimide agar, the diagnosis was confirmed. <i>Camellia sinensis</i> silver nanoparticles (CAGNPs) were created using an extract of the plant's aqueous and methanolic leaves. Based on the results of the nanoparticle synthesis, spherical nanoparticles that may be single or mixed were included in both the aqueous and methanolic extracts of silver nanoparticles. By comparing their retention times to those of the reference compounds, the HPLC findings revealed that two phenolic compounds (gallic acid and caffeine) had been discovered. Utilising the disc diffusion technique, the antibacterial activity of (CAGNPs) was assessed. The results indicated that the methanolic (CAGNPs) extract was more effective than the aqueous (CAGNPs) extract at 375 and 750 ppm, giving the highest inhibition zone 17.67 and 21.33 mm, respectively, when compared to the aqueous (CAGNPs) extract, which produced inhibitory zones 13.00 and 16.33 mm, respectively. The MIC findings indicated that the methanolic CAGNPs extract was more effective than the aqueous CAGNPs extract; the MIC of the methanolic CAGNPs extract was 23.43 µg/ml in all <i>P. aeruginosa</i> isolates, except the isolates No. 9 and 10, which was 11.718 µg/ml. While in the aqueous extract, the MIC in all <i>P. aeruginosa</i> isolates was 187.5 µg/ml, with the exception of isolates No. 9 and 10, which was 93.75 µg/ml. Additionally, the methanolic CAGNPs extract entirely inhibited <i>P. aeruginosa</i> from building a biofilm when used at 23.43 µg/ml. However, at 46.87 µg/ml of the aqueous CAGNPs extract, totally reduced the biofilm forming activity on <i>P. aeruginosa</i> isolates.
Keywords <i>P. aeruginosa</i> <i>C. sinensis</i> Nanoparticles Antibacterial Antibiofilm	
*Corresponding Author: ahmed@ige.uobaghdad.edu.iq	

INTRODUCTION

Public health is seriously threatened by the advent of microorganisms that are widely drug-resistant, or non-susceptible to all but one or two antibiotic classes, and multidrug-resistant, or resistant to three or more antibiotic classes (Liu, Wu, Zhu, 2022). Bacterial drug resistance contributed to 4.95 million deaths globally in 2019 (AL-Azawi, 2017). One of the most important worldwide risks to human and animal health, food safety and security, and economic and agricultural growth is the quick generation and spread of resistant bacteria (Larsen *et al.*, 2022). Additionally, because of their propensity to create biofilms, which shields them from the immune system of the host, antibiotics, and disinfectants, bacteria are a significant contributor to chronic and recurring infections (Yasin, AL-Azawi, 2019). Therefore, it is now more crucial than ever to create a novel, potent treatment strategy in order to eliminate and manage resistant bacteria.

Recent advances in nanotechnology have made it possible to utilize nanoparticles as biological agents to prevent the growth of bacteria (Singh *et al.*, 2021). The size of nanoparticles, which range from 1 to 100 nm, is very tiny, and they have a high surface energy. They are appropriate for a variety of industrial applications, including the chemical, pharmaceutical, mechanical, and food processing industries, thanks to these special qualities (Koca *et al.*, 2022). Metal-based nanoparticles such as silver, gold, platinum, nickel, manganese, titanium, and zinc have non-toxic and antibacterial properties (Yang *et al.*, 2015). For the synthesis of NPs, many approaches based on physical, chemical, biological, and hybrid processes can be applied. Physical and chemical approaches have several drawbacks, such as being expensive, relying heavily on dangerous chemicals, requiring complicated equipment, and having difficult synthesis conditions (Ying *et al.*, 2022). Due to their eco-friendliness, cost-effectiveness, safe handling, biocompatibility, and a wide variety of metabolites with antioxidant and antimicrobial activities, green synthesis methods of nanoparticles are receiving a lot of attention lately as an alternative to traditional chemical and physical methods (Khalaf *et al.*, 2021). Ag-NPs have therefore had extensive application as antibacterial agents due to their remarkable antibacterial properties (MO, Zhou, He, 2022).

MATERIALS AND METHODS

Bacterial Isolates

Ten isolates of *P. aeruginosa* were obtained from the genetic engineering and biotechnology institute/University of Baghdad. These isolates were previously identified by molecular and chemical testing after being gathered from many hospitals in Baghdad. The isolates were incubated at 42°C for 18–24 hours on cetrinide agar, and use the VITEK-2 in order to confirm the diagnosis. After being re-cultured on nutrient agar medium to bring them back to life, the isolates were incubated aerobically at 37°C for 24 hours.

Collection of *Camellia sinensis* L.

The *C. sinensis* that was bought from the city's markets was recognised as *C. sinensis* L. by a specialist from the biology department of the Faculty of Science / University of Baghdad. Plant leaves were cleaned and let to air dry in order to create *C. sinensis* extract. An electric lab grinder was used to reduce the plant leaves to a powder. First, the fat was extracted by macerating 200 g of *C. sinensis* leaves in 1 liter of petroleum ether solvent. The residue was made in two batches, air-dried, and gathered. Aqueous and methanolic extracts were made from each batch of defatted plant leaves independently using methanol and water. Two distinct extraction bottles containing methanol alcohol, one litre (L) of sterile distilled de-ionized water, and every 200 g of powdered plant material was used. After then, the combinations were kept of three days in a dark area, occasionally being stirred each day to guarantee even mixing and extraction. By allowing it to evaporate at 37°C, the filtrate was concentrated. Subsequently, the samples were placed in an amber tube and stored at 4°C (Sskatawa *et al.*, 2021).

Biosynthesis of nanoparticles by extracts of *Camellia sinensis*

According to Alazzawi, Ghaloub, Yaaqoob, 2023, with modification, Five milliliters of each extract were sprayed dropwise, independently, under ultrasonic conditions using 95 milliliters of a 10 mM silver nitrate AgNO₃ solution were subjected to a power of 100 W and a frequency of 42 kHz. Following a 20-minute sonication, the solutions were stored for 48 hours at 25°C in opaque vials. To separate the clear supernatant, the reaction mixture was centrifuged for 10 minutes at 10,000 rpm after being stirred for 30 minutes at 800 rpm for 24 hours. After 24 h the reaction mixture was purified by centrifugation for 10 min at 10000 rpm to get a clear supernatant.

Samples of the most recent colloid were stored at 4°C in opaque containers. Over the course of five days, liquids containing *C. sinensis* and silver nanoparticles (CAGNPs) underwent a colour change, which is indicative of the AgNPs' formation.

Characterization of the prepared nanoparticles

In this work, a variety of methods were used to describe the morphological and structural properties of CAGNPs in order to identify Ag-NPs.

UV-Visible Absorption Spectroscopy

The reduction of the Ag ions in the colloidal solution was shown using UV-visible spectroscopy (UV-Vis). The wavelength was scanned between (200-800) nm using a tiny aliquot of Ag NPs in a quartz cuvette, with clean water serving as the reference. The UV-Vis absorption spectra of the sample were obtained using a Perkin Elmer Spectrophotometer at various intervals 5, 10, 15, and 20 minutes after adding *C. sinensis* extract to a Silver nitrate solution (Elbossaty, 2017).

Fourier Transform Infrared (FTIR) Spectroscopy Analysis

The functional groups that plant extracts produced on the surface of Ag-NPs were characterised by FTIR analysis (Shimadzu). At a resolution of 4 cm⁻¹, and in the 400 to 4000 cm⁻¹ range, the spectra were scanned. As is customary, the samples were created by spreading them out on a glass slide. After then, the material was examined (Ashraf *et al.*, 2018).

Atomic force microscopy

Using 100 microliters of each kind of nanoparticle sample, a thin layer was made on a glass slide, and it was allowed to dry for five minutes. The Atomic force microscopy (AFM) was then used to scan the slides (Hammodi, Rashid, Oraibi, 2019).

High-Performance Liquid Chromatography (HPLC)

High-Performance Liquid Chromatography (HPLC) was used to detect methanolic and aqueous (CAGNPs) extract preparations, according to Radovanovic *et al.*, (2015).

Antibiotic susceptibility test

The World Health Organisation (2003). recommends the Kirby-Bauer technique, which was used to assess the susceptibility of twelve different antibiotics. To create a bacterial suspension with a moderate turbidity in relation to the standard turbidity solution (5 x 10⁸ CFU per millilitre), 1-2 isolated bacterial colonies from the original culture were put to a test tube containing 4 ml of normal saline. A part of the bacterial solution was transferred, dispersed uniformly, and gently spread over Mueller-Hinton agar medium using a sterile cotton swab. It was then incubated for ten minutes. After that, the antimicrobial discs were firmly applied to the surface. The plates were then turned over and let to sit at 37 °C for 18 to 24 hours. A metric ruler was used to measure the inhibition zones that developed around the discs in accordance with the Clinical Laboratories Standards Institute CLSI (2019).

Evaluation of biofilm production

The capability of *P. aeruginosa* to quantitatively generate biofilms was assessed in accordance with guidelines Patel, Goswami, Khara (2016). Each isolate was cultivated for one night at 37 °C in Brain Heart Infusion Broth. After that, the isolates were added to 1% glucose-containing tryptic soy broth (TSB) and pipetted until well mixed. To satisfy the turbidity criterion of McFarland No. 0.5, the bacterial isolate solution was modified accordingly.

Every isolate's culture was moved to a sterile 200 µl flat-bottom microplate with 96 wells. After placing the covers on the plates, they were incubated aerobically for 24 hours at 37°C. The planktonic cells were twice rinsed with distilled water after the incubation period in order to remove any bacteria that hadn't attached. The adherent bacterial cells in each well were fixed with 200 µl of 100% methanol for 20 minutes at room temperature. Each well was filled with 200 µl of crystal violet 0.1%, the adhering cells were stained for 15 minutes. Following the completion of the staining process, further stains were eliminated by frequently (2-4 times) washing with distilled water. To ensure they were totally dry, the plate was let to stand at room temperature for about half an hour. Ultimately, the discoloration was removed using 33% acetic acid. After that, optical density (OD) measurements were collected at 630 nm using an ELISA auto reader. Three separate replications of each experiment were carried out in triplicate. In addition, a cut-off value (Odc) was established. It is defined as three standard deviations (SD) above the mean OD of the negative control: Odc = average OD of negative control + (3 × SD of negative control). The isolates were classified into the four following categories based upon the OD: non-

biofilm producer ($OD < OD_c$); weak-biofilm producer ($OD_c < OD < 2 \times OD_c$); moderate-biofilm producer ($2 \times OD_c < OD < 4 \times OD_c$); strong-biofilm producer ($4 \times OD_c < OD$) (Kirmusaoglu, 2019).

Examine the antibacterial properties of the compound (CAgNPs)

Method of disc diffusion

The methanolic and aqueous (CAgNPs) extracts were evaluated for antibacterial activity using the disc diffusion method, as reported by Razmavar *et al.*, (2014).

Using a sterile swab, the *P. aeruginosa* were uniformly spread on Muller Hinton agar plates (0.5 McFarland). The plates were dried for 15 minutes before to the sensitivity test. The final concentrations of 375 ppm and 750 ppm of the methanolic and aqueous (CAgNPs) extracts was used. Then, 20 μ l of each dilution were impregnated onto 6 mm diameter sterile blank discs.

DMSO discs and distil water were used as control. Prior to placement on the Mueller Hinton agar surface, all discs were completely dried. The plates were incubated at 37°C for 18 to 24 hours. Throw using the diameter of the inhibitory zone surrounding the discs after incubation, the antibacterial activity was calculated. To assure dependability, each test was run three times.

Examination of the minimum inhibitory concentration (MIC) of the compound (CAgNPs)

The broth microdilution technique was used on a 96-well microtiter plate to measure the Minimum Inhibitory Concentration (MIC) of the compound (CAgNPs) extracts. The working solution for the (CAgNPs) extracts was prepared in broth at a concentration of 375 μ g/ml. Two-fold dilutions of the extract were performed immediately on the plate for the methanolic and aqueous (CAgNPs) extracts, yielding concentrations of (2.92, 5.85, 11.718, 23.43, 46.87, 93.75, 187.5, and 375) μ g/ml. One hundred microliters of the produced methanolic and aqueous (CAgNPs) extracts were placed into the first wells in row A. In rows B through H, each column had only 100 μ l of broth. A micropipette was used to apply double serial dilutions sequentially along the columns beginning with rows A through H. Repeating the process up to row (H), the last 100 μ l were discarded. 100 μ l of broth was taken from the starting concentrations in row A, mixed properly, and added to the subsequent row. As a consequence, all test wells containing extracts are lowered to 100 μ l in volume, with the exception of the column, which retained 200 μ l of the sterility control broth. Except for the negative control, all wells received the 1.5×10^8 CFU/ml bacterial inoculum injection. For 18 to 20 hours, microtiter plates were incubated at 37°C. Each well received 20 μ l of the resazurin dye. The minimum concentration of extracts visible in broth microdilutions was established to be the lowest concentration at which no colour shifted from blue to pink (Ohikhena, Wintola, Afolayan, 2017).

Study the antibiofilm activity of the compound (CAgNPs)

Utilising a 96-well microtiter plate, the anti-biofilm activity of the methanolic (CAgNPs) and aqueous (CAgNPs) extracts was assessed. Plant extract working solutions were prepared at the following concentrations: 375, 187.5, 93.7, 46.87, 23.43, 11.718, 5.85, and 2.92 μ g/ml. Only the first wells in row A contained 100 μ l of each sample, and only rows B through H had 100 μ l of the broth. Twofold serial dilutions were made progressively down the columns, starting with rows A through H, using a micropipette. Once the procedure was repeated up to the last row (H), the remaining 100 μ l were removed. After being well mixed, 100 μ l of the starting concentrations in row A were taken out and transported to the following row. 100 μ l of the 1×10^8 CFU/ml bacterial inoculum was applied to each well, except the negative control. Assessment of biofilm formation was done using the exact same procedure as was mentioned in (**Evaluation of biofilm production**).

Statistical analysis

The Statistical Analysis System-SAS programmed was utilized to determine how various study parameter influences were made. In this study, a significant comparison between means was made using the least significant difference (LSD) test.

RESULTS

Nanoparticle biosynthesis and characterization

UV-Visible spectroscopy

The use of UV-visible spectroscopy to validate the synthesis of Ag-NPs and the color shift is a crucial step. The colour altered when AgNO₃ aqueous solution was mixed with *C. sinensis* extract. Free electrons in the silver nanoparticles collectively vibrate in resonance with the light wave, resulting in a colour change and a unique peak value. Figures 1 and 2 displays the UV-visible spectra of plant extracts with and without AgNO₃ solution, the weak absorption peak at 200 nm indicates the presence of a variety of chemical substances that are known to interact with silver ions.

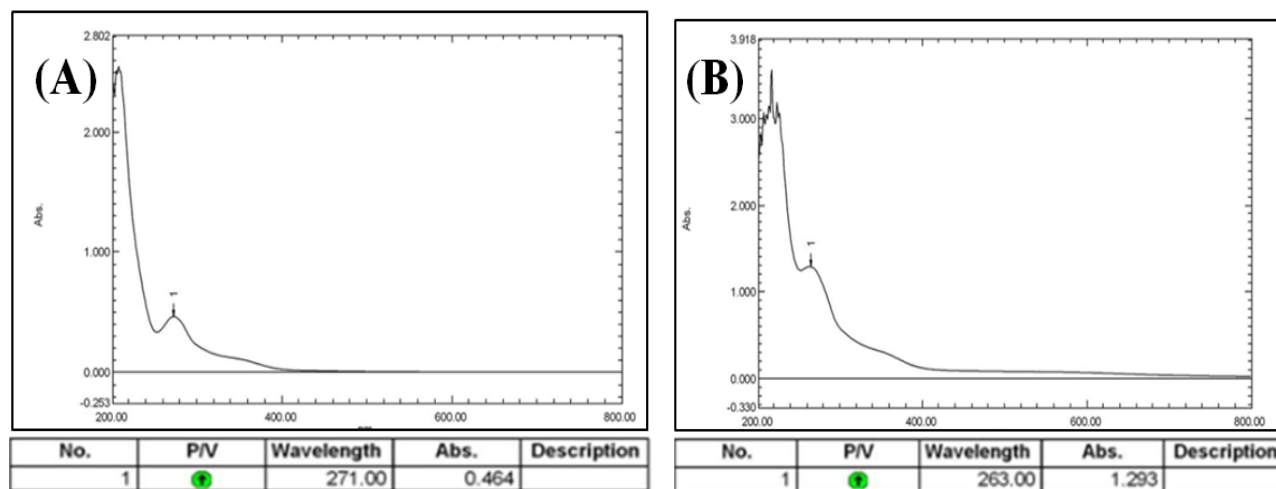


Figure 1: Analysis of the UV-Visible spectrum of (A): Aqueous extract of *C. sinensis*, (B): synthesised aqueous (CAgNPs) extract

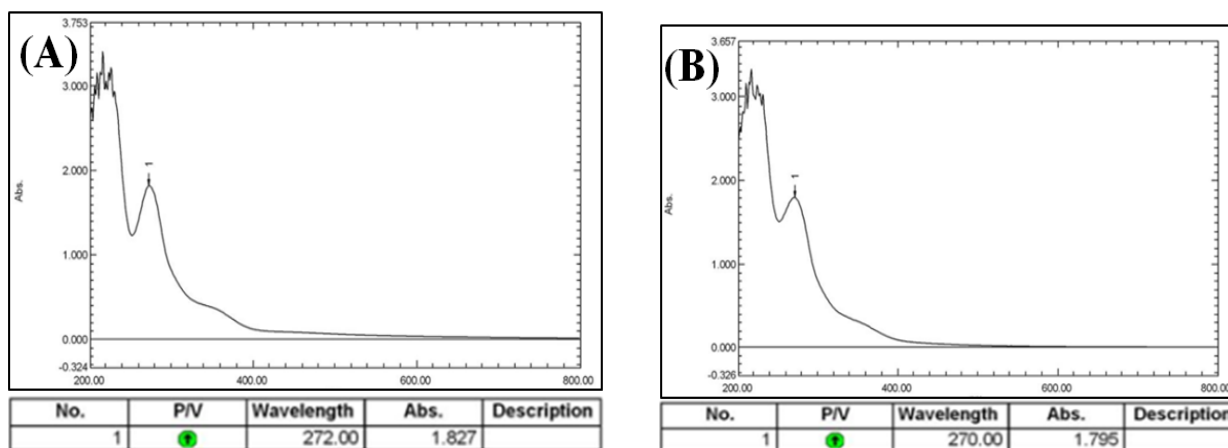


Figure 2: Analysis of the UV-Visible spectrum of (A): Methanolic extract of *C. sinensis*, (B): synthesised methanolic (CAgNPs) extract synthesised *Rosemary officinalis* (RAgNPs) methanolic extract

Fourier transformation infrared spectroscopy (FTIR)

FTIR examination of the produced *C. sinensis* leaves extract revealed the plant extract's dual action as a bio-reduction and capping agent. Spectrums between 4000 and 670 cm^{-1} (2.5 and 15 μm), or occasionally as low as 200 cm^{-1} (50 μm), range were recorded using Fourier Transform Infrared (FTIR) spectrophotometers. A number of functional groups, including C-H stretching, N-H bend, C-C stretching, and C-N stretching, were detected in the FTIR spectra of the methanolic and aqueous extracts of *C. sinensis*. Additionally, bands of absorbance were visible at peaks (394.73, 2935.66, 1695.43, 1448.54, and 1018.42) cm^{-1} for the methanolic extract and (3417.87, 2358.94, 1637.57, 1448.55, and 1041.57) cm^{-1} for the aqueous extract (Table 1). The aqueous (CAgNPs) extract exhibited absorbance bands at (3421.73, 2937.58, 2358.93, 1643.36, 1369.47, and 1037.71) cm^{-1} , while the methanolic (CAgNPs) extract featured prominent absorbance bands at peaks (3433.28, 1649.15, 1373.33, and 1029.98) cm^{-1} , according to FTIR spectroscopy (Figure 3 and 4).

Table 1: IR frequencies region for the functional groups of the *C. sinensis* extracts

The Functional Group	I.R wave number Standard groups	I.R wave number of methanolic extract	I.R wave number of aqueous extract	I.R wave number of methanolic (CAgNPs) extract	I.R wave number of aqueous (CAgNPs) extract
Phenolic-OH groups stretching	3650-2500	3940.73	3417.87	3433.28	3421.73
C-H stretching	2960-2850	2935.67	2358.94	-----	2937.58
N-H band	1650-1580	1695.43	1637.57	1649.15	1643.36
C-C stretching	1500-1400	1448.83	1448.55	-----	-----
C-N stretching	1250-1020	1018.42	1041.57	1029.98	1037.71

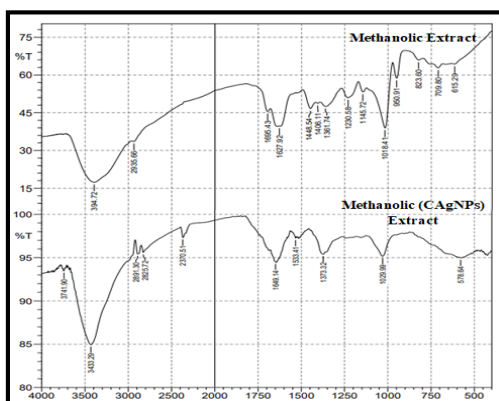


Figure 3: FTIR Spectral Pattern of the methanolic extracts of *C. sinensis* and (CAgNPs)

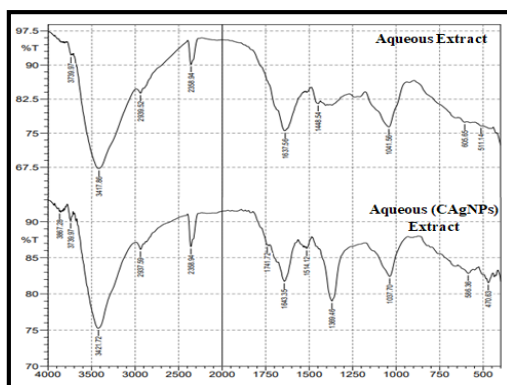


Figure 4: FTIR Spectral Pattern of the aqueous extracts of *C. sinensis* and (CAgNPs)

Atomic force microscopy (AFM)

According to the AFM analysis the methanolic CAgNPs and aqueous CAgNPs extracts had average particle sizes of 84.77 nm and 108.4 nm, respectively as shown in (Figures 5 and 6).

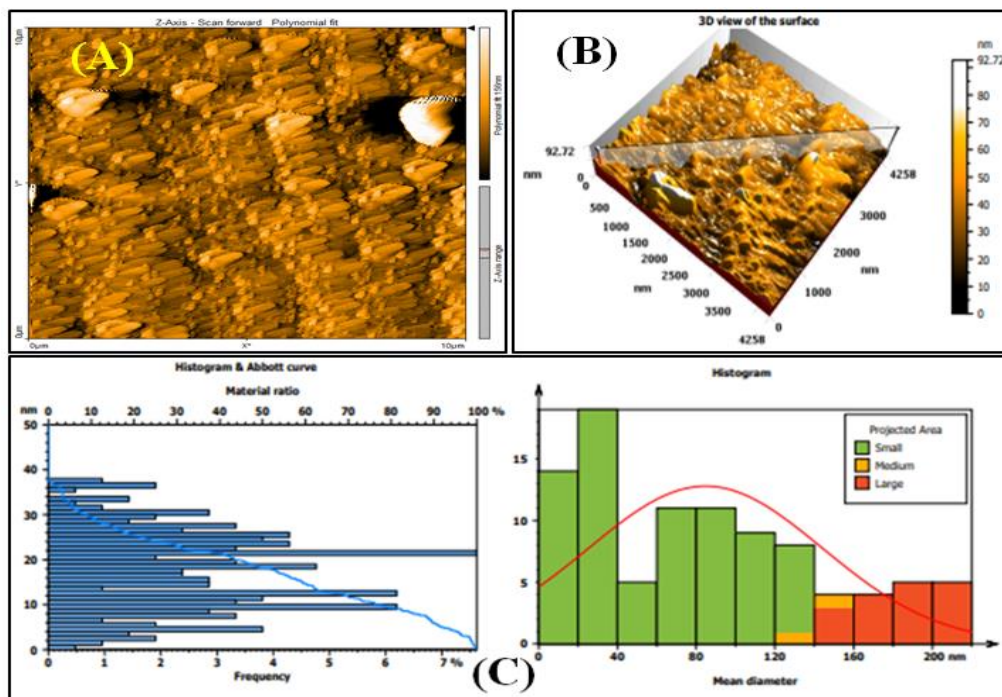


Figure 5: AFM evaluation of the methanolic CAgNPs extract (A): 2-D of methanolic CAgNPs extract, (B): 3-D of methanolic CAgNPs extract, (C): AFM graphic showing the methanolic extract of CAgNPs size range.

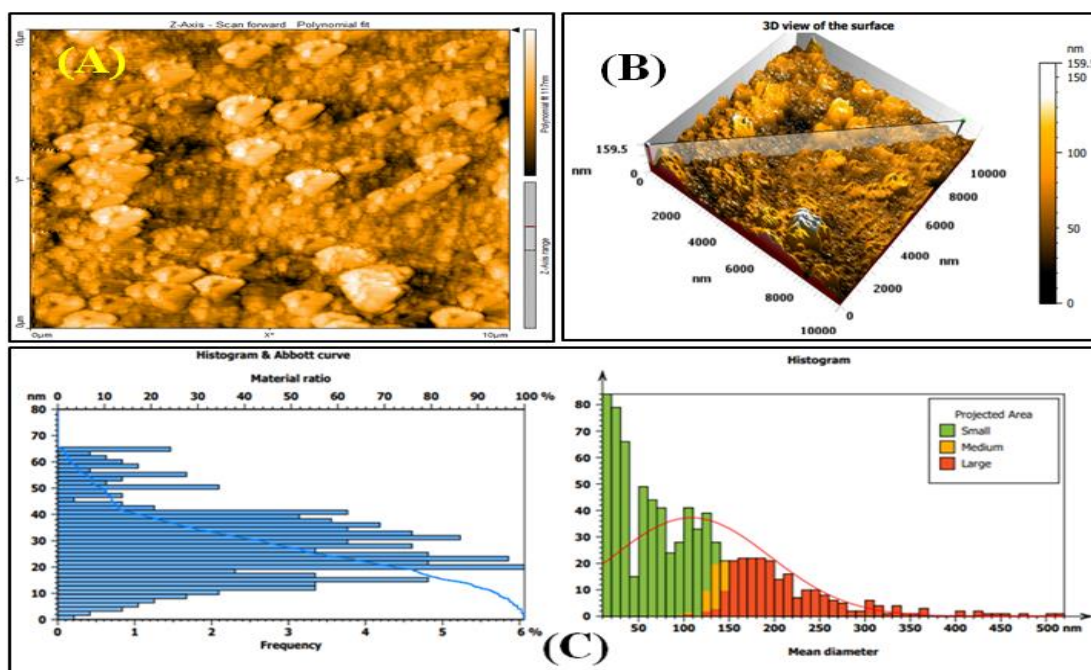


Figure 6: AFM evaluation of the aqueous CAgNPs extract (A): 2-D of aqueous CAgNPs extract, (B): 3-D of aqueous CAgNPs extract, (C): AFM graphic showing the aqueous extract of CAgNPs size range.

High-performance liquid chromatography (HPLC)

The individual phenol contents of CAgNPs were examined using the HPLC method, as reported by Radovanovic *et al.*, (2015). The present study revealed the presence of two phenolic compounds, namely caffeine and gallic acid, in the methanolic CAgNPs extract and aqueous CAgNPs extract (Figures 7 and 8), when compared to standard compounds (Figure 9).

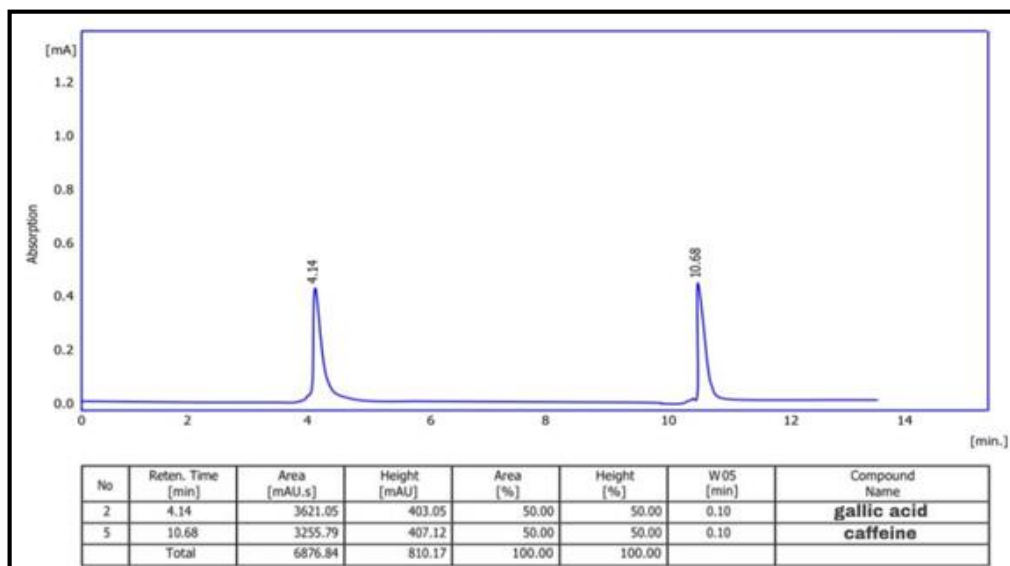


Figure 7: HPLC chromatogram of phenol compounds in methanolic (CAgNPs) extract

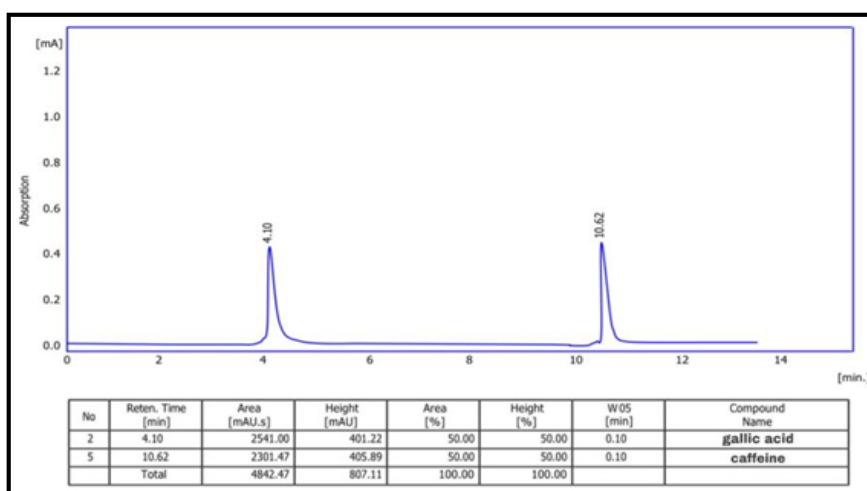


Figure 8: HPLC chromatogram of phenol compounds in aqueous (CAgNPs) extract

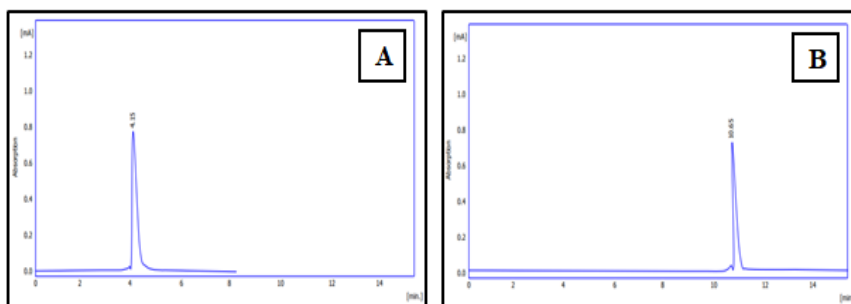


Figure 9: HPLC chromatogram of phenol compound standards (A): gallic acid, (B): caffeine

Antibiotic susceptibility test

The following 12 antibiotics were tested on all 10 isolates of *P. aeruginosa*: Ticarcillin, Piperacillin, Imipenem, Tobramycin, Piperacillin, Ceftazidime, Gentamicin, Cefepime, Meropenem, Colistin, Amikacin, and Ciprofloxacin. The research revealed that *P. aeruginosa* isolates typically exhibited extraordinarily high levels of drug resistance to the treatments used in this study as shown in (Table 2).

Table 2: Antibiotic sensitive test on clinical isolates of *P. aeruginosa*

Antibiotic	T I C	P R L	I M I	T O B	P R Z	C A Z	G N	C F M	M E R	C O	A K	C I P	Resistance %
Isolate													
P ₁	R	R	R	R	R	R	R	R	R	R	R	R	100%
P ₂	R	R	R	R	R	R	R	R	R	S	R	R	91.6%
P ₃	R	R	R	S	R	R	S	R	R	S	R	R	75%
P ₄	R	R	S	R	R	R	R	R	R	S	R	R	83.33%
P ₅	R	R	R	S	R	R	S	R	R	S	R	R	75%
P ₆	R	R	R	R	R	R	R	R	R	S	R	R	91.33%
P ₇	R	R	R	R	R	R	R	R	R	S	R	R	91.66%
P ₈	R	R	R	R	R	R	R	R	R	S	R	R	91.66%
P ₉	R	R	R	S	R	R	S	S	R	R	R	R	75%
P ₁₀	R	R	R	R	R	R	R	S	R	R	R	R	91.66%

(P): *Pseudomonas aeruginosa*, (TIC): Ticarcillin, (PRL): Piperacillin, (IMI): Imipenem, (TOB): Tobramycin, (PRZ): Piperacillin / Tazobactam, (CAZ): Ceftazidime, (GN): Gentamycin, (CFM): Cefepime, (MER): Meropenem, (CO): Colistin, (AK): Amikacin, (CIP): Ciprofloxacin.

Detection of biofilm Formation

Using the microtiter plate method, the quantitative formation of the biofilms is quantified, and absorbance at 630 nm is detected by an ELISA reader. The optical density of isolates ranges from 0.215 to 0.622, or 0.435 to 0.287 on average. According to result in (Table 3) showed that 100% of the isolates were capable of producing strong biofilms.

Table 3: Isolates of *P. aeruginosa* producing biofilms

<i>P. aeruginosa</i> isolates	P ₁	P ₂	P ₃	P ₄	P ₅	P ₆	P ₇	P ₈	P ₉	P ₁₀

(P):

Biofilm forming	Stro ng	Stro ng	Stro ng	Stro ng	Stro ng	Stro ng	Stro ng	Stro ng	Stro ng	Stro ng	Stro ng
No. of Isola te	Methanolic (CAgNPs) extract		Aqueous (CAgNPs) extract		LSD value						
	375 (ppm)	750 (ppm)	375 (ppm)	750 (ppm)							
<i>P</i> ₁	14.67 ± 0.58	18.67 ± 0.58	11.33 ± 0.58	15.33 ± 0.58	1.582 **						
<i>P</i> ₂	14.33 ± 0.58	18.33 ± 0.58	10.33 ± 0.58	14.33 ± 0.58	1.582 **						
<i>P</i> ₃	13.00 ± 1.00	17.33 ± 0.58	10.00 ± 1.00	13.33 ± 1.16	2.623 **						
<i>P</i> ₄	14.33 ± 0.58	18.33 ± 0.58	10.33 ± 0.58	14.00 ± 1.00	1.937 **						
<i>P</i> ₅	12.67 ± 0.58	17.33 ± 0.58	10.67 ± 0.58	13.33 ± 0.58	1.582 **						
<i>P</i> ₆	13.67 ± 0.58	18.33 ± 0.58	11.33 ± 0.58	13.67 ± 3.22	4.612						
<i>P</i> ₇	13.33 ± 0.58	17.33 ± 0.58	10.33 ± 0.58	13.00 ± 1.73	2.740 **						
<i>P</i> ₈	13.67 ± 1.16	18.67 ± 0.58	11.33 ± 0.58	14.33 ± 0.58	2.092 **						
<i>P</i> ₉	16.67 ± 0.58	20.67 ± 0.58	13.00 ± 0.00	16.33 ± 0.58	1.370 **						
<i>P</i> ₁₀	17.67 ± 0.58	21.33 ± 0.58	12.33 ± 0.58	15.33 ± 0.58	1.582 **						
LSD value	1.643 **	1.341 **	1.407 **	3.088	----						
** (P≤0.01)											

Pseudomonas aeruginosa, Control negative (cut off) = 0.13

Antibacterial properties of (CAgNPs) extracts

Method of disc diffusion

The disk-diffusion technique was used to assess the antibacterial activity of (CAgNPs) extracts on *P. aeruginosa* isolates. Table (4) shows that at dosages of 375 and 750 ppm, In comparison to the aqueous (CAgNPs) extract, the methanolic (CAgNPs) extract demonstrated greater efficacy. It produced the highest inhibition zone in *P. aeruginosa*, which were 17.67 and 21.33 mm, respectively, when compared to the aqueous (CAgNPs) extract, which produced inhibition zones 13 and 16.33.

Table 4: Antibacterial activity of (CAgNPs) methanolic and aqueous extracts *P. aeruginosa* isolates

Isolate	Silver nanoparticles aqueous extract	Silver nanoparticles methanolic extract
	MIC (µg/ml)	MIC (µg/ml)
<i>P</i> ₁	187.5	23.43
<i>P</i> ₂	187.5	23.43
<i>P</i> ₃	187.5	23.43
<i>P</i> ₄	187.5	23.43
<i>P</i> ₅	187.5	23.43
<i>P</i> ₆	187.5	23.43
<i>P</i> ₇	187.5	23.43
<i>P</i> ₈	187.5	23.43
<i>P</i> ₉	93.75	11.718
<i>P</i> ₁₀	93.75	11.718

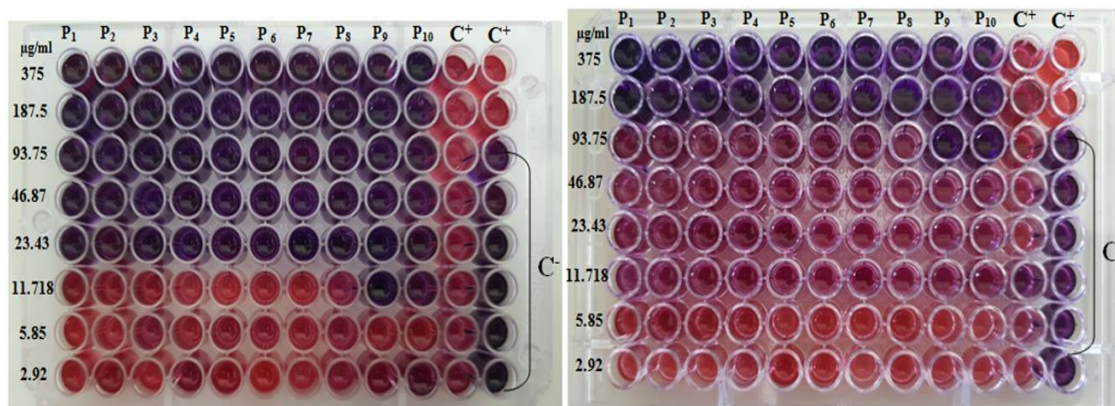
The numbers in the table mention to inhibition zone measured in (mm)

The (MIC) of the CAgNPs extracts

Using the broth microdilution method on a microtiter plate with 96 wells, the MIC of the CAgNPs extracts was determined. One method to determine the minimum inhibitory concentration (MIC) of antimicrobial drugs against *P. aeruginosa* is to utilise the oxidation-reduction colorimetric indicator resazurin. The MIC results demonstrated the greater effectiveness of the methanolic CAgNPs extract over the aqueous CAgNPs extract. All *P. aeruginosa* isolates exhibited MIC values of 23.43 µg/ml for the methanolic CAgNPs extract, as shown in (Table 5) and Figures (10 and 11), with the exception of isolates No. 9 and 10, which was 11.718 µg/ml. Also With the exception of isolates No. 9 and 10, which showed MIC 93.75 µg/ml for the aqueous CAgNPs extract, all *P. aeruginosa* isolates had MIC 187.5 µg/ml.

Table 5: MIC of CAgNPs methanolic and aqueous extracts on *P. aeruginosa* isolates

(P): *P. aeruginosa* isolate



(P): *P. aeruginosa* isolate, (C⁺): Control positive (Bacteria + Media), (C⁻): Control negative (Media only) (P): *P. aeruginosa* isolate, (C⁺): Control positive (Bacteria + Media), (C⁻): Control negative (Media only)

Figure 10: MIC of methanolic CAgNPs extract on *Pseudomonas aeruginosa*

Figure 11: MIC of aqueous CAgNPs extract on *Pseudomonas aeruginosa*

Anti-Biofilm Activity of CAgNPs extracts

The methanolic CAgNPs extract entirely inhibited 100% of the *P. aeruginosa* producing a biofilm at a concentration of 23.43 µg/ml, and 70% when used at 11.718 µg/ml, as shown in (Table 6). However, the aqueous CAgNPs extract completely decreased the biofilm forming activity of *P. aeruginosa* isolates in a concentration 46.87 µg/ml, as shown in Table 7.

Table 6: Biofilm formation of *Pseudomonas aeruginosa* before and after treatment with methanolic CAgNPs extract

No of isolates	Before treatment	After treatment with silver nanoparticles methanolic extract (µg/ml)							
		2.92	5.85	11.718	23.43	46.87	93.75	187.5	375
P ₁	Strong	Moderate	Weak	No Biofilm					
P ₂	Strong	Moderate	Moderate	Weak	No Biofilm				
P ₃	Strong	Moderate	Weak	No Biofilm					
P ₄	Strong	Weak	Weak	Weak	No Biofilm				
P ₅	Strong	Weak	Weak	No Biofilm					
P ₆	Strong	Weak	No Biofilm						
P ₇	Strong	Moderate	No Biofilm						
P ₈	Strong	Weak	Weak	Weak	No Biofilm				
P ₉	Strong	Moderate	No Biofilm						
P ₁₀	Strong	Weak	Weak	No Biofilm					

Table 7: Biofilm formation of *Pseudomonas aeruginosa* before and after treatment with aqueous CAgNPs extract

No of isolates	Before treatment	After treatment with silver nanoparticles aqueous extract (µg/ml)							
		2.92	5.85	11.718	23.43	46.87	93.75	187.5	375
P ₁	Strong	Moderate	Moderate	Moderate	No Biofilm				
P ₂	Strong	Moderate	Weak	Weak	No Biofilm				
P ₃	Strong	Moderate	Moderate	Moderate	No Biofilm				
P ₄	Strong	Moderate	Moderate	Weak	No Biofilm				
P ₅	Strong	Moderate	Moderate	Weak	No Biofilm				
P ₆	Strong	Strong	Strong	Moderate	No Biofilm				
P ₇	Strong	Moderate	Moderate	No Biofilm					
P ₈	Strong	Moderate	Moderate	Moderate	Weak	No Biofilm	No Biofilm	No Biofilm	No Biofilm
P ₉	Strong	Moderate	Weak	No Biofilm					
P ₁₀	Strong	Moderate	Moderate	Moderate	Moderate	No Biofilm	No Biofilm	No Biofilm	No Biofilm

DISCUSSION

The AgNPs were made using aqueous and methanolic extracts of *C. sinensis*. Plant extracts can more easily and successfully produce metallic nanoparticles than other bio-reductants

(Arokiyaraj *et al.*, 2017). It is well known that these highly stable nanoparticles are produced by phytochemicals that not only cap Ag⁺ but also convert it to Ag⁰ (Salleh *et al.*, 2020). In this work, the formation of silver nanoparticles was monitored by UV spectroscopy absorption and colour change. When *C. sinensis* extracts, both methanolic and aqueous, were added, the green AgNPs solutions for CAgNPs underwent colour changes. After 24 hours, the color started to shift, and it took 48 hours for the color to reach its ultimate state. The methanolic and aqueous extracts of *C. sinensis* contain active molecules, indicating that the formation of (AgNPs) was likely the result of the conversion of Ag metal ions Ag⁺ into Ag⁰ nanoparticles. Plant metabolites, including proteins, carbohydrates, phenols, terpenoids, alkaloids, and flavonoids, are essential for the stability and transformation of metallic Ag into (AgNPs). By prolonging the incubation period, particle formation and decay can be accelerated, leading to an increase in colour intensity with longer reaction times (Saliem, Ibrahim, Salih, 2016). The colour change is brought on by the surface Plasmon resonance (SPR) activation of the metal nanoparticles. One of the fascinating optical properties of Ag-NPs is directly connected to the great control of localised SPR by the NPs form (Femi-Adepoju, 2019). This outcome is in line with the findings of Saleh and Najim (2020), who showed the potential for color change when silver ions were converted into silver nanoparticles after coming into contact with plant extracts. Ag-NPs characterization is therefore essential for evaluating the functional characteristics of the generated particles. For a number of studies, the preferred reducing biomaterial was leaf extract from *C. sinensis*. The present research's findings were in close agreement with those of a study he did with Al-Khafaji and AL-Azawi (2022).

Plasmon resonance absorbance is highly dependent on the kind, size, and shape of the produced NPs as well as temperature, dielectric constant, and other factors in the medium (Mohammed, Al-jubouri, 2019). The 200–800 nm range was used to measure the absorption spectra. The silver surface Plasmon resonance band is centred at 263.00 nm in the aqueous (CAgNPs) extract and 270.00 nm in the methanolic (CAgNPs) extract when compared to the UV Test findings for *C. sinensis*, which are 271.00 and 272.00 nm, respectively. Using UV-vis spectroscopy, an SPR peak at the same wavelength was found during a stability analysis of biologically produced AgNPs that lasted more than a year (Zhang *et al.*, 2016).

Silver nitrate reduction/bio-reduction and stabilization of AgNO₃ may be caused by functional groups, which were found using Fourier transformation infrared spectroscopy (FTIR). A technique for determining the vibration frequencies of molecular bonding is called FTIR spectroscopy. Based on the band value in the infrared radiation area, it is used to confirm the presence of the functional groups of the active ingredients in the synthesised Ag-NPs (Saad *et al.*, 2021). The CAgNPs spherical in shape, either singly or in aggregates, in both two-dimensional and three-dimensional perspectives This result was consistent with that of Bhat *et al.*, (2021) who observed that the almost spherical silver nanoparticles produced by biosynthesis were either solitary (25–50 nm) or found in clusters (100 nm).

According to the antibiotic susceptibility of the tested isolates, all of *P. aeruginosa* isolates were multi-drug resistant. According to Saderi and Owlia (2015), this skill can be either innate or acquired by horizontal gene transfer or genetic material modification. As a result of antibiotic misuse, *P. aeruginosa* has developed resistance to a variety of antibiotics, causing an increase in antibiotic resistance and antibiotic cross-resistance, as well as the emergence of *P. aeruginosa* multi-drug resistant (MDR) strains (Yayan, Ghebremedicalhin, Rasche, 2015). One of the most important aspects of *P. aeruginosa*'s pathogenicity is its ability to create biofilms; this eventually causes persistent infections and encourages bacterial survival in a range of settings, including burn wounds (De Almeida Silva *et al.*, 2017). Previous studies have demonstrated a connection between *P. aeruginosa*'s multidrug resistance phenotype and its capacity to form biofilms (Yekani *et al.*, 2017).

The antibacterial activities of CAgNPs extracts may be due to the secondary metabolites present in the methanol extracts. For instance, polyphenols (flavonoids and phenols) have been found to have antimicrobial properties (Adeeyo *et al.*, 2021). Invading the bacterial cell, the phenolic chemicals disrupt cellular metabolism. Additionally, they associate with the cell's enzymes in

active areas to work to lock them up, preventing them from remaining in contact with the fundamental substances. Adenosine triphosphate (ATP) is an oxidising agent that is bound by any reducing agent. This prevents ATP from being used as an energy source, weakening the energy in the microbial cell whether it be bacterial or fungal decreasing its efficacy, and ultimately causing its death (Fathima, Rao, 2016). Numerous phenolic compounds have antibacterial properties against plant diseases that can also be used to combat infections that affect humans. Additionally, many derived phenolic compounds' antibacterial activity employ pathways distinct from those of traditional medicines, which suggest they may be crucial for advancing antibacterial treatment (Sanver *et al.*, 2016). Thus, the high concentration of phenolic components (caffeine and gallic acid) found in the aqueous and methanolic extracts of CAgNPs is related to the antibacterial activity seen in this study. The antibacterial activity of the CAgNPs extracts was very strong against isolates of *P. aeruginosa*. Additionally, due to their size, they can readily access bacterial nuclei and exhibit a sizable and outstanding surface area, which is where contact with bacteria is most intense. In addition, it is assumed that the AgNPs' reduced size may have allowed them to bind to the bacterial cell membrane's surface and interfere with important processes including permeability and respiration. Then it might have easily entered the bacterium and caused more harm, maybe by interacting with substances containing sulphur and phosphorus, such as DNA, leading to cell lysis. The size, shape, surface, surface charge, solubility, exposure period, and concentration all affect how the AgNPs interact with bacterial cultures (Espinosa *et al.*, 2020). Nanoparticles have been shown to be in contact with bacterial cell walls to achieve successful antibacterial function. The forms of contact may be through hydrophobic interactions, electrostatic attraction and van der Waals forces (Hassan, Mahmood, 2019). It is clear that as the particle size is reduced to the nanoscale range, a dosage of nanoparticles has a bigger specific surface area, allowing for more material contact with the environment, such as the cell membrane of the targeted pathogenic bacteria.

A biofilm is a small group of microbial cells that colonies both living and inanimate surfaces and encase themselves in polymers released by the microbes. It can occasionally be challenging to treat diseases caused by biofilms that are multidrug resistant (Kumar, Chhibber, Harjai, 2013). Therefore, it is essential to find brand-new, powerful compounds that prevent the growth of bacterial biofilms. The inhibition of biofilm growth through the use of a concentration-dependent technique evinced the capacity of phenolic compounds to reduce biofilm formation. Because flavonoids partially lyse the bacteria, they presumably promote bacterial aggregation. A lowered membrane surface can only absorb a specific quantity of active nutrients as a result of the membrane fusion (Laith, AL-Azawi, 2022). Numerous mechanisms of phenolic antibacterial activity have been identified, such as interactions between bacterial proteins and cell walls, damage to cytoplasmic membranes, a reduction in membrane fluidity, and inhibition of energy metabolism, nucleic acid synthesis, or cell wall synthesis (Daglia, 2012). Comparatively, studies on plant phenolic anti-biofilm activity have demonstrated that these compounds have "softer" effects that suppress biofilms without affecting bacterial growth by interfering with bacterial regulatory systems such as quorum sensing or other global regulator systems (Silva, Zimmer, Macedo, 2016) Moreover, gallic acid penetration by the biofilm killed *S. aureus*, as reported by Liu *et al.* (2017). Furthermore, biofilm development in bacterial isolates is significantly impacted by Ag-NPs green production (Shakerimoghaddam *et al.*, 2020). According to the results of this study, methanolic *C. sinensis* extract nanoparticles had a greater level of biological activity against *P. aeruginosa* than aqueous extract nanoparticles. This may be because the methanolic extract has higher levels of phenolic compounds both quantitatively and qualitatively than the aqueous extract, and these phytochemicals may be responsible for the various antibacterial properties.

CONCLUSION

The results of the present investigation provide evidence in favor of the effective production of CAgNPs by green synthesis employing methanolic and aqueous leaf extracts of *C. sinensis*. The synthesized CAgNPs exhibit potent antibacterial effects against *P. aeruginosa* and, depending on the dose utilized, can also prevent the growth of *P. aeruginosa* biofilms. This study also found that

phenolic compounds isolated from *C. sinensis* leaves and present in CAgNPs have antibacterial and anti-biofilm effects on *P. aeruginosa*.

FUNDING: The authors received no specific funding for this work.

CONFLICT OF INTEREST DISCLOSURE: The authors declare no conflict of interest.

REFERENCES

- Adeeyo AO, Edokpayi JN, Alabi MA, Msagati TA, Odiyo JO. Plant active products and emerging interventions in water potabilisation: disinfection and multi-drug resistant pathogen treatment. *Clinical Phytoscience*. 2021; 7(1), 1-16. doi.org/10.1186/s40816-021-00258-4.
- AL-Azawi AH. Phytochemical, Antibacterial and Antioxidant Activities of *dodonea viscosa* Jacq. extracts Cultivated. *Iraqi Journal of Biotechnology*. 2017; 16(4): 37-46.
- Alazzawi AA, Ghaloub AN, Yaaqoob LA. Investigating the Antioxidant and Apoptosis Inducing Effects of Biologically Synthesized Silver Nanoparticles Against Lymphoma Cells in Vitro. *Iraqi Journal of Science*. 2023; 4390-4403. DOI: 10.24996/ij.s.2023.64.9.9.
- Al-Khafaji AR, Al-Azawi AH. Green Method Synthesis of Silver Nanoparticles Using Leaves Extracts of *Rosmarinus officinalis*. *Iraqi journal of biotechnology*. 2022; 21(2), 251-267.
- Arokiyaraj S, Vincent S, Saravanan M, Lee Y, Oh YK, Kim KH. Green synthesis of silver nanoparticles using *Rheum palmatum* root extract and their antibacterial activity against *Staphylococcus aureus* and *Pseudomonas aeruginosa*. *Artificial cells, nanomedicine, and biotechnology*. 2017; 45(2), 372-379. <https://doi.org/10.15739/ibspr.18.005>.
- Ashraf A, Zafar S, Zahid K, Salahuddin M, Al-Ghanim KA, Al-Misned F. Synthesis, characterization, and antibacterial potential of silver nanoparticles synthesized from *Coriandrum sativum* L. *J Infect Public Health*. 2019; 12(2):275-81. doi: 10.1016/j.jiph.2018.11.002, PMID 30477919.
- Bhat M, Chakraborty B, Kumar RS, Almansour AI, Arumugam N, Kotresha D, Nayaka S. Biogenic synthesis, characterization and antimicrobial activity of *Ixora brachypoda* (DC) leaf extract mediated silver nanoparticles. *Journal of King Saud University-Science*. 2021; 33(2), 101296. doi:10.1016/j.jksus.2020.101296.
- Clinical Laboratory Standards Institute (CLSI). Performance Standards for Antimicrobial Susceptibility Testing; CLSI Supplement, CLSI M100-28th ed., Clinical and Laboratory Standards Institute Wayne, PA, U.S.A. 2019; 39(1).
- Daglia M. Polyphenols as antimicrobial agents. *Current opinion in biotechnology*. 2012; 23(2), 174-181. DOI: 10.1016/j.copbio.2011.08.007.
- De Almeida Silva KCF, Calomino MA, Deutsch G, De Castilho SR, De Paula GR, Esper LMR. Molecular characterization of multidrug resistant (MDR) *Pseudomonas aeruginosa* isolated in a burn center. *Burns*. 2017; 43: 137-143. DOI: 10.1016/j.burns.2016.07.002
- Elbossaty WF. Green tea as biological system for the synthesis of silver nanoparticles. *J. biotechnol. biomater.* 2017; 7(269): 2. doi:10.4172/2155-952X.1000269.
- Espinosa JCM, Cerritos RC, Morales MAR, Guerrero KPS, Contreras RAS, Crystals JM. Characterization of silver nanoparticles obtained by a green route and their evaluation

- in the bacterium of *Pseudomonas aeruginosa*. Crystals. 2020; 10(5): 13. doi.org/10.3390/cryst10050395.
- Fathima A, Rao JR. Selective toxicity of Catechin-a natural flavonoid towards bacteria. Applied Microbial Biotechnology. 2016; 100:6395-6402. DOI: 10.1007/s00253-016-7492-x.
- Femi-Adepoju AG, Dada AO, Otun, KO, Adepoju AO, Fatoba OP. Green synthesis of silver nanoparticles using terrestrial fern (*Gleichenia Pectinata* (Willd.) C. Presl.): characterization and antimicrobial studies. Heliyon. 2019; 5(4). DOI: 10.1016/j.heliyon.2019.e01543.
- Hammodi HF, Rashid IH, Oraibi AG. Green biosynthesis, Identification and characterization of Ag and Zn nanoparticles using Ivy (*Epipremnum aureum*) plant extract. Plant Arch. 2019; 19(2):959-65. https://doi.org/10.1016/j.kijoms.2017.10.007.
- Hassan DF, Mahmood MB. Biosynthesis of Iron Oxide Nanoparticles Using *Escherichia coli*. Iraqi Journal of Science. 2019; 60(3): 453-459. DOI: 10.24996/ijs.2023.64.5.11.
- Khalaf RL, Ahmed EM, Mathkor TH, Al-Zubaidi HY. Synthesis of Silver Nanoparticles Using L.RosaFlowers Extracts: Thermodynamic and Kinetic Studies on the Inhibitory Effects of Nanoparticles on Creatine Kinase Activity. Iraqi Journal of Science. 2021; vol. 62, no. 8, pp. 2486-2500. doi.org/10.24996/ijs.2021.62.8.1.
- Kirmusaoglu S. The Methods for Detection of Biofilm and Screening Antibiofilm Activity of Agents. In Exopolysaccharides Methods of Preparation and Application. In technology Open. 2019; DOI: http:// dx.doi.org / 10.5772 / intechopen.84411.
- Koca FD, Halici MG, İşik Y, Ünal G. Green Synthesis of Ag-ZnO Nanocomposites by Using *Usnea Florida* and *Pseudevernia Furfuracea* Lichen Extracts and Evaluation of Their Neurotoxic Effects. Inorg. Nano Metal Chem. 2022; 1-8. doi: 10.1080/24701556.2022.2078351.
- Kumar L, Chhibber S, Harjai K. Zinger one inhibits biofilm formation and improve Antibiofilm efficacy of ciprofloxacin against *Pseudomonas aeruginosa* PAO1. Fitoterapia. 2013; 90: 73-78. DOI: 10.1016/j.fitote.2013.06.017.
- Laith FM, AL-Azawi AH. Antibiofilm Activity of *Conocarpus erectus* Leaves Extract and Assessment Its Effect on *pelA* and *algD* Genes on Multi-drug Resistant *Pseudomonas aeruginosa*. The Egyptian Journal of Hospital Medicine. 2022; 89 (2): 6961- 6969. DOI: 10.21608/EJHM.2022.271919.
- Larsen J, Raisen CL, Ba X, Sadgrove NJ, Padilla-González GF, Simmonds MSJ, Loncaric I, Kerschner H, Apfalter P, Hartl R. Emergence of Methicillin Resistance Predates the Clinical Use of Antibiotics. Nature. 2022; 602:135-141. doi: 10.1038/s41586-021-04265-w.
- Liu M, Wu X, Li J, Liu L, Zhang R, Shao D, Du X. The specific anti-biofilm effect of gallic acid on *Staphylococcus aureus* by regulating the expression of the *ica* operon. Food Control. 2017; 73: 613-618. https://doi.org/10.1016/j.foodcont.2016.09.015.
- Liu X, Wu Y, Zhu Y. Emergence of colistin-resistant hypervirulent *Klebsiella pneumoniae* (CoR-HvKp) in China. Emerg Microbes Infect. 2022; 11(1):648-661. doi: 10.1080/22221751.2022.2036078.
- Mo F, Zhou Q, He Y. Nano-Ag: environmental applications and perspectives. Sci Total Environ. 2022; 829:154644. doi: 10.1016/j.scitotenv.2022.154644.

- Mohammad DAE, Al-Jubouri SHK. Comparative antimicrobial activity of silver nanoparticles synthesized by *Corynebacterium glutamicum* and plant extracts. *Baghdad Sci. J.* 2019; 16(3 Suppl.): 689-696. DOI:[http://dx.doi.org/10.21123/bsj.2019.16.3 \(Suppl.\).0689](http://dx.doi.org/10.21123/bsj.2019.16.3 (Suppl.).0689).
- Ohikhena FU, Wintola OA, Afolayan AJ. Evaluation of the Antibacterial and Antifungal Properties of *Phragmanthera capitata* (Sprengel) Balle (Loranthaceae), a Mistletoe Growing on Rubber Tree, Using the Dilution Techniques. *The Scientific World Journal.* 2017; Article ID 9658598. 8 pages. doi.org/10.1155/2017/9658598.
- Patel FM, Goswami PN, Khara R. Detection of Biofilm formation in device associated clinical bacterial isolates in cancer patients. *Sri Lankan Journal of Infectious Diseases.* 2016; 6(1): 43-50. DOI: 10.4038/sljid.v6i1.8086.
- Radovanovic B, Mladenovic J, Radovanovic A, Pavlovic R, Nikolic V. Phenolic composition, antioxidant, antimicrobial and cytotoxic activities of *Allium porrum* L. (Serbia) extracts. *Journal of Food and Nutrition Research.* 2015; 3(9), 564-569. DOI: 10.12691/jfnr-3-9-1.
- Razmavar S, Mahmood AA, Salmah BI, Pouya H. Antibacterial Activity of Leaf Extracts of *Baeckea frutescens* against Methicillin-Resistant *Staphylococcus aureus*. *BioMedical Research International.* 2014. Article ID 521287, 5 pages. doi.org/10.1155/2014/521287.
- Saad AM, El-Saadony MT, El-Tahan AM, Sayed S, Moustafa MA, Taha AE, Ramadan MM. Polyphenolic extracts from pomegranate and watermelon wastes as substrate to fabricate sustainable silver nanoparticles with larvicidal effect against *Spodoptera littoralis*. *Saudi Journal of Biological Sciences.* 2021; 28(10), 5674-5683. doi: 10.1016/j.sjbs.(2021).06.011, PMID 34588879.
- Saderi H, Owlia P. Detection of multidrug resistant (MDR) and extremely drug resistant (XDR) *P. aeruginosa* isolated from patients in Tehran, Iran. *Iranian journal of pathology.* 2015; 10: 265. PMID: PMC4539747.
- Saleh GM, Najim SS. Antibacterial activity of silver nanoparticles synthesized from plant latex. *Iraqi Journal of Science.* 2020; 1579-1588. DOI:10.24996/ij.s.2020.61.7.5.
- Saliem AH, Ibrahim OM, Salih SI. Biosynthesis of Silver Nanoparticles using *Cinnamon zeylanicum* Plants Bark Extract. *Kufa j. vet. Sci.* 2016; 7(1):51- 63. <https://doi.org/10.1155/2022/4894642>.
- Salleh A, Naomi R, Utami ND, Mohammad AW, Mahmoudi E, Mustafa N, Fauzi MB. The potential of silver nanoparticles for antiviral and antibacterial applications: A mechanism of action. *Nanomaterials.* 2020; 10(8), 1566. <https://doi.org/10.3390/nano10081566>.
- Sanver D, Murray BS, Sadeghpour A, Rappolt M, Nelson AL. Experimental modeling of flavonoid bio-membrane interactions. *Langmuir.* 2016; 32:13234-13243. doi.org/10.1021/acs.langmuir.6b02219.
- Shakerimoghaddam A, Razavi D, Rahvar F, Khurshid M, Ostadkelayeh SM, Esmaeili SA. Evaluate the effect of zinc oxide and silver nanoparticles on biofilm and *icaA* gene expression in methicillin-resistant *Staphylococcus aureus* isolated from burn wound infection. *Journal of Burn Care and Research.* 2020; 41(6): 1253-1259. doi: 10.1093/jbcr/iraa085.

- Silva LN, Zimmer KR, Macedo AJ, Trentin DS. Plant natural products targeting bacterial virulence factors. *Chemical reviews*. 2016; 116(16): 9162-9236. doi.org/10.1021/acs.chemrev.6b00184.
- Singh KR, Nayak V, Singh J, Singh AK, Singh RP. Potentialities of Bioinspired Metal and Metal Oxide Nanoparticles in Biomedical Sciences. *RSC Adv*. 2021; 11:24722–24746. doi: 10.1039/D1RA04273D.
- Ssekatawa K, Byarugaba D, Kato C, Nakavuma J, Wampande E, Ejobi F, Nxumalo E. Physiochemical properties and antibacterial activity of silver nanoparticles green synthesized by *Camellia sinensis* and *Prunus africana* extracts. *Research square*. January 21; 2021. DOI: https://doi.org/10.21203/rs.3.rs-143995/v1.
- World Health Organization (WHO), *Basic laboratory procedures in clinical bacteriology*. 2nd ed. Geneva, Switzerland. 2003.
- Yang X, Yang M, Pang B, Vara M, Xia Y. Gold Nanomaterials at Work in Biomedicine. *Chem. Rev*. 2015; 115:10410–10488. doi: 10.1021/acs.chemrev.5b00193.
- Yasin SA, and AL-Azawi AH. Antibacterial Activity of *Conocarpus Erectus* Leaves Extracts on Some Microorganisms Isolated From Patients With Burn Infection. *Plant Archives*. 2019; 19(2): 583-589.
- Yayan J, Ghebremedicalhin B, Rasche K. Antibiotic resistance of *Pseudomonas aeruginosa* in pneumonia at a single university hospital center in Germany over a 10-year period. *Plos one*. 2015; 10: 1-20. DOI: 10.1371/journal.pone.0139836.
- Yekani M, Memar MY, Alizadeh N, Safaei N, Ghotaslou R. Antibiotic resistance patterns of biofilm-forming *Pseudomonas aeruginosa* isolates from mechanically ventilated patients. *International Journal of Scientific Study*. 2017; 5(5): 84-88. DOI: 10.17354/ijssl/2017/106.
- Ying S, Guan Z, Ofoegbu PC, Clubb P, Rico C, He F, Hong J. Green Synthesis of Nanoparticles: Current Developments and Limitations. *Environ. Technol. Innov*. 2022; 26:102336. doi: 10.1016/j.eti.2022.102336.
- Zhang XF, Liu ZG, Shen W, Gurunathan S. Silver nanoparticles: synthesis, characterization, properties, applications, and therapeutic approaches. *International journal of molecular sciences*. 2016; 17(9), 1534. DOI: 10.3390/ijms17091534.